Journal of Volcanology and Geothermal Research 433 (2023) 107734

Contents lists available at ScienceDirect

Journal of Volcanology and Geothermal Research

journal homepage: www.journals.elsevier.com/journal-of-volcanology-and-geothermal-research

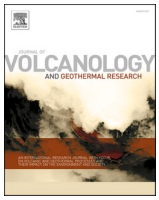

Space-time analysis of informational properties of GPS time series recorded at the Campi Flegrei caldera (Italy)

Simona Tripaldi [a,*], Michele Lovallo [b], Marilena Filippucci [a], Luciano Telesca [c]

[a] Dipartimento di Scienze della Terra e Geoambientali, Università degli Studi di Bari Aldo Moro, Campus Universitario, via Orabona 4, 70125 Bari, Italy
[b] Agenzia Regionale per la Protezione dell'Ambiente della Basilicata, 85100 Potenza, Italy
[c] Institute of Methodologies for Environmental Analysis, National Research Council, 85050 Tito, Italy

ARTICLE INFO

Keywords:
Shannon entropy power
Fisher information measure
Complexity
GPS time series
Campi Flegrei caldera

ABSTRACT

In this work the time dynamics of GPS time series recorded at the Campi Flegrei caldera from 2000 to 2019 was investigated by using the Fisher Information Measure (FIM) and the Shannon entropy power (SEP), two informational methods that allow the detection of changes in the dynamical behavior of a complex system, like the volcanic one, quantifying respectively the order/organization and the disorder/uncertainty. By jointly analyzing the FIM and the SEP through the Fisher-Shannon Information Plane (FSIP) it was shown that the SEP discriminates quite well the vertical displacement time series, while the FIM discriminates better the horizontal ones, which are featured by a more complex behavior. Globally, the most striking change in the SEP is found in 2012, while at local scale abrupt loss of order (indicated by low values of FIM) well correlate with the occurrence of seismic swarms. A further informational quantity, the complexity C (given by the product between SEP and FIM), has been revealed to be sensitive to the baseline deformation level increases and to the small-amplitude modulation of deformation signals within the caldera.

1. Introduction

Horizontal and vertical deformations of the Earth's crust are widely used to monitor volcanic activity. The displacement pattern before and after an eruption may indicate the depth and rate of magma accumulation as well as the way magma is accommodated (Dvorak and Dzurisin, 1997). Together with seismicity and degassing, deformation is a good indicator of volcanic unrest. Monitoring these observables in unrest context elucidates the behavior and the working principles within a volcano, contributing to forecast activity (Acocella et al., 2015).

The Campi Flegrei caldera (CFc, Southern Italy), a volcanic complex mainly formed during the Campanian Ignimbrite (CI, 39 ka) and the Neapolitan Yellow Tuff (NYT, 15 ka) eruptions (De Vivo et al., 2001; Deino et al., 2004), is well known for ground level variations since roman times. The last CFc eruption occurred in 1538 CE, was preceded by a rapid uplift of 6–7 m and by increased seismicity, and lead to the formation of Monte Nuovo. Early record of vertical displacement at CFc are based on historical documents and on Roman ruins studies.

Recordings made after 1819 above the floor of the Roman Temple of Serapeum, in the city of Pozzuoli, and the first precise leveling measures of Campi Flegrei in 1905 report the sinking at the center of the caldera (Dvorak and Mastrolorenzo, 1991; Parascandola, 1947). Since then, intermittent unrest has been accompanied by uplifts phases. During 1950–1952, a 0.73 m uplift occurred and, although the seismic surveillance wasn't yet activated, no seismicity with magnitude higher than 1.5 has been supposed (Del Gaudio et al., 2010). Between 1969 and 1972 moderate seismicity accompanied an uplift of 1.77 m, while during the 1982–1984 crisis an uplift of 1.79 m was accompanied by >16,000 earthquakes often clustered in swarms (D'Auria et al., 2011; De Natale and Zollo, 1986; Del Gaudio et al., 2010); this crisis led to the evacuation of nearly 40,000 people in October 1983 (Barberi et al., 1984). Thereafter, a slow subsidence followed until 2005, when a new uplift phase restarted and is still ongoing. Minor peaks of uplift ((Gaeta, 2003; Troise et al., 2019) occurred both during the post-1984 subsidence and the recent uplift (1989, 1994, 2000, 2006 and 2012–2013). On October 2006 a LP (long period) seismic sequence occurred with >300 events recorded and located at about 500 m depth, beneath the Solfatara crater (Ricco et al., 2019). The VT (volcano tectonic) activity shows alternating phases of intense swarms with phases with very low seismicity rate ((Petrosino et al., 2018). Major seismic swarms composed of up to 200 earthquakes, with duration magnitude Md up to 2.5, were observed in October 2005, October 2006, January 2008, March 2010, September

* Corresponding author.
E-mail address: simona.tripaldi@uniba.it (S. Tripaldi).

https://doi.org/10.1016/j.jvolgeores.2022.107734
Received 7 June 2022; Received in revised form 30 November 2022; Accepted 11 December 2022
Available online 14 December 2022

2012, March 2014, October 2015, July 2016, August 2016, March 2018, September 2018 and October 2018 with the most energetic earthquakes since 2005 occurred in October 2015 (Md = 2.5), July 2016 (Md = 2.1), March 2018 (Md = 2.4), September 2018 (Md = 2.5) and October 2018 (Md = 2.0) (Ricco et al., 2019).

Due to the intense urbanization of the CFc area, the volcanic risk management lead to the intensification of the monitoring activities through time. Continuous GPS measurements are made since 2000 by the "Neapolitan Volcanoes Continuous GPS" (NeVoCGPS) network, part of the geodetic monitoring system operating at the INGV-Osservatorio Vesuviano (Bottiglieri et al., 2010; De Martino et al., 2014). Nowadays, the NeVoCGPS network comprises 21 on land GPS stations in the CFc area (De Martino et al., 2021). From 2000 to 2019, the vertical displacement recordings show a bell-shaped patter, with the largest uplift detected by the RITE station located at Rione Terra–Pozzuoli; the horizontal displacement recordings show a radial pattern centered on Pozzuoli (De Martino et al., 2021). These patterns were already observed in studies concerning previous unrest crises (Berrino et al., 1984; De Natale and Pingue, 1993).

The origin of ground deformation at CFc has been the subject of intense research, leading to different source/sources models. Some authors have interpreted the ground deformation as the signature of pressure/volume source changes or shallow intrusion of magmatic origin (Berrino et al., 1984; Bianchi et al., 1987; D'Auria et al., 2015; Trasatti et al., 2015). Alternative interpretations point to fluid-dynamical perturbations in the hydrothermal system and to the influence of the rock's properties, like permeability (Battaglia et al., 2006; Bonafede and Mazzanti, 1998; Lima et al., 2009; Petrillo et al., 2019; Todesco et al., 2010). The observed displacements are the expression of superimposed processes that may occur at different time and space scales. The extraction of information about the different sources driving ground deformation can be afforded also by statistical approaches (Dong et al., 2002; Gualandi et al., 2016). At CFc, GPS time series have been analyzed by applying independent component analysis (ICA) recognizing the background deformation level and the periodic signals associable to Earth tides (Bottiglieri et al., 2010; Bottiglieri et al., 2007). ICA applied to tiltmetric recordings also highlighted tidal contribution components likely controlled by structural and thermoelastic site properties (De Lauro et al., 2018). Via a purely statistical approach, GPS together with seismicity and geochemical data have been analyzed to explore inter-relation structure of the multivariate time series and unrest geo-indicators (Tripaldi et al., 2020).

In this work we analyze the time dynamics of deformation data recorded by the "Neapolitan Volcanoes Continuous GPS" network in the CFc in the time span 2000–2019 by employing the statistical tools Fisher Information Measure (FIM) and Shannon entropy (SEP). FIM and SEP were initially formulated in the context of the information theory and then have been finding successful application in the analysis of complex dynamics of nonstationary time series (Guignard et al. (2020) and herein references) and, in particular, in the analysis of dynamical changes in geophysical signals. Earthquake-related significant changes were found in the time variation of FIM and SEP of geoelectrical signals measured in seismically active areas (Telesca et al., 2005). Precursory signs of volcanic eruptions were detected by analyzing the time distribution of FIM and SEP of satellite thermal signals recorded at Mt. Etna, Italy (Lovallo et al., 2009; Lovallo et al., 2007). Investigating the seismic tremor measured at Stromboli volcano, Italy (Telesca et al., 2010), and at El Hierro volcano, Spain (Telesca et al., 2014a), onsets eruptive phases were revealed by applying the FIM. Long-term deformation processes of the Taiwan orogeny were identified by using the Fisher-Shannon method applied to geoelectrical data (Telesca et al., 2014b). The FIM and SEP were also employed to elucidate laboratory and theoretical models of earthquake rupture models (Chen et al., 2021; Moreno-Torres et al., 2018; Wu et al., 2019).

Here we focus on the Fisher-Shannon analysis of vertical (V) and horizontal (H) components of displacement of GPS signals measured in the volcanic caldera of Campi Flegrei in order to identify a spatial pattern of the stations depending on the distance from the supposed source and to evidence dynamical changes in the time variation of the signals that are linked with unrest phases.

2. Data and methods

2.1. Data

In this study we investigate the daily time series of displacements recorded by the GPS NeVoCGPS network at CFc and downloaded by (De Martino et al., 2021). For a detailed description of data recording and processing see De Martino et al., (De Martino et al., 2021; De Martino et al., 2014). Among all the stations of the GPS network, we selected only those stations with the longest recording period; the analysis was performed on the vertical (V) and horizontal (H) components from August 2000 to December 2019; in particular the H component was the modulus of the sum between north and east components. Fig. 1 shows the location of GPS stations and the analyzed time series. From a visual inspection, the highest vertical displacements are recorded at the station RITE that is close to the caldera center and to the Solfatara hydrothermal system (Fig. 1).

2.2. Fisher–Shannon method

The Fisher Information Measure (FIM) and the Shannon entropy (SE) are generally used to investigate the informational properties of a time series. In information theory, these two quantities quantify the degree of smoothness of the distribution of a series, and are also employed to explore the complexity of nonstationary series described in terms of order and organization (FIM) or disorder and uncertainty (SE) (Frieden, 1990; Shannon, 1948). The FIM and SE are defined by the following formulae:

$$\mathrm{FIM} = \int_{-\infty}^{+\infty} \left(\frac{\partial}{\partial x} f(x)\right)^2 \frac{dx}{f(x)} \tag{1}$$

$$\mathrm{SE} = -\int_{-\infty}^{+\infty} f_X(x) log f_X(x) dx \tag{2}$$

where $f(x)$ is the probability density function of the series x. Since SE can also be negative, it is generally used the Shannon entropy power (SEP) N_X defined by

$$SEP = \frac{1}{2\pi e} e^{2H_X} \tag{3}$$

As it can be seen from the definitions (Eq. (1) and (2)), the FIM and SE characterize the local and global properties of $f(x)$, respectively. The FIM and SEP are not independent of each other, since between them the isoperimetric inequality $\mathrm{FIM} \cdot N_X \geq D$, where D is the dimension of the space, is held (Esquivel et al., 2010).

Reliable values of FIM and SEP follow an accurate estimate of the $f(x)$. In this paper, we use the kernel-based approach for estimating FIM and SE that was demonstrated to perform better than the discrete-based approach (Telesca and Lovallo, 2017). Thus, after applying the kernel density estimator method (Devroye, 1987; Janicki and Weron, 1994).

$$\widehat{f}_M(x) = \frac{1}{Mb} \sum_{i=1}^{M} K\left(\frac{x - x_i}{b}\right) \tag{4}$$

where M and b are respectively the length of the series and the bandwidth, while $K(u)$ is the Gaussian kernel

$$\widehat{f}_M(x) = \frac{1}{M\sqrt{2\pi b^2}} \sum_{i=1}^{M} e^{-\frac{(x-x_i)^2}{2b^2}} \tag{5}$$

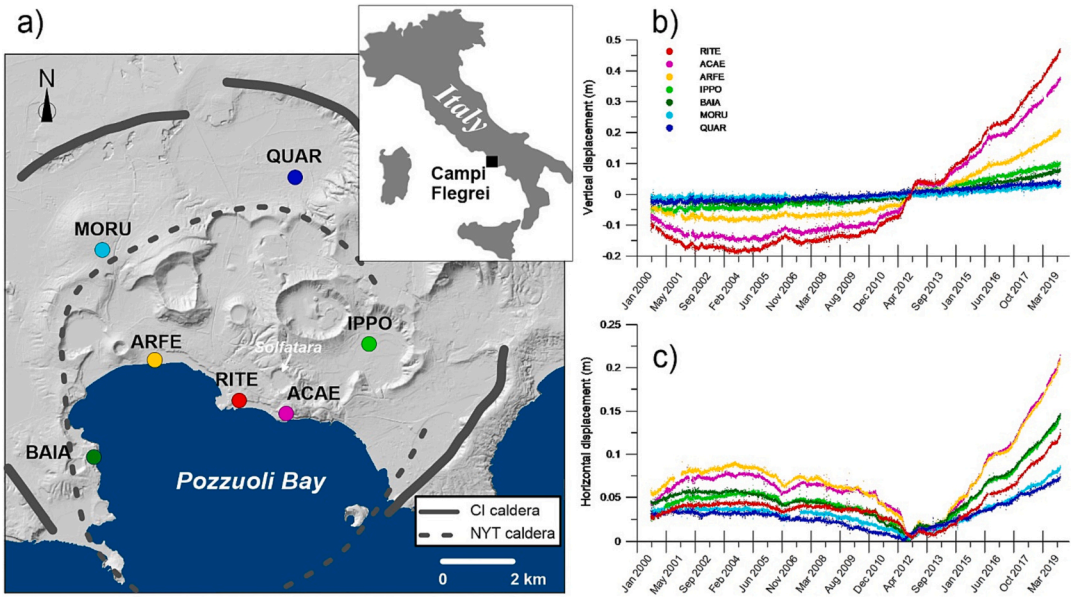

Fig. 1. Map of the Campi Flegrei caldera and location of GPS stations (colored filled circles) considered in the present work (a), vertical (b) and horizontal (c) displacements. CI: Campanian Ignimbrite; NYT: Neapolitan Yellow Tuff. (For interpretation of the references to colour in this figure legend, the reader is referred to the web version of this article.)

$f(x)$ is estimated through an optimization method that integrates the algorithms of Troudi et al. (Troudi et al., 2008) and that of Raykar and Duraiswami (Raykar and Duraiswami, 2006). The time dynamics of the series can be investigated representing the series in the so-called Fisher-Shannon information plane (FSIP), whose coordinate axes are *SEP* and FIM. For 1-D time series, the hyperbolic curve $FIM \cdot SEP = 1$ separates the FSIP into two parts, of which only the space $FIM \cdot SEP \geq 1$ is admissible due to the isoperimetric inequality. Any time series can be represented

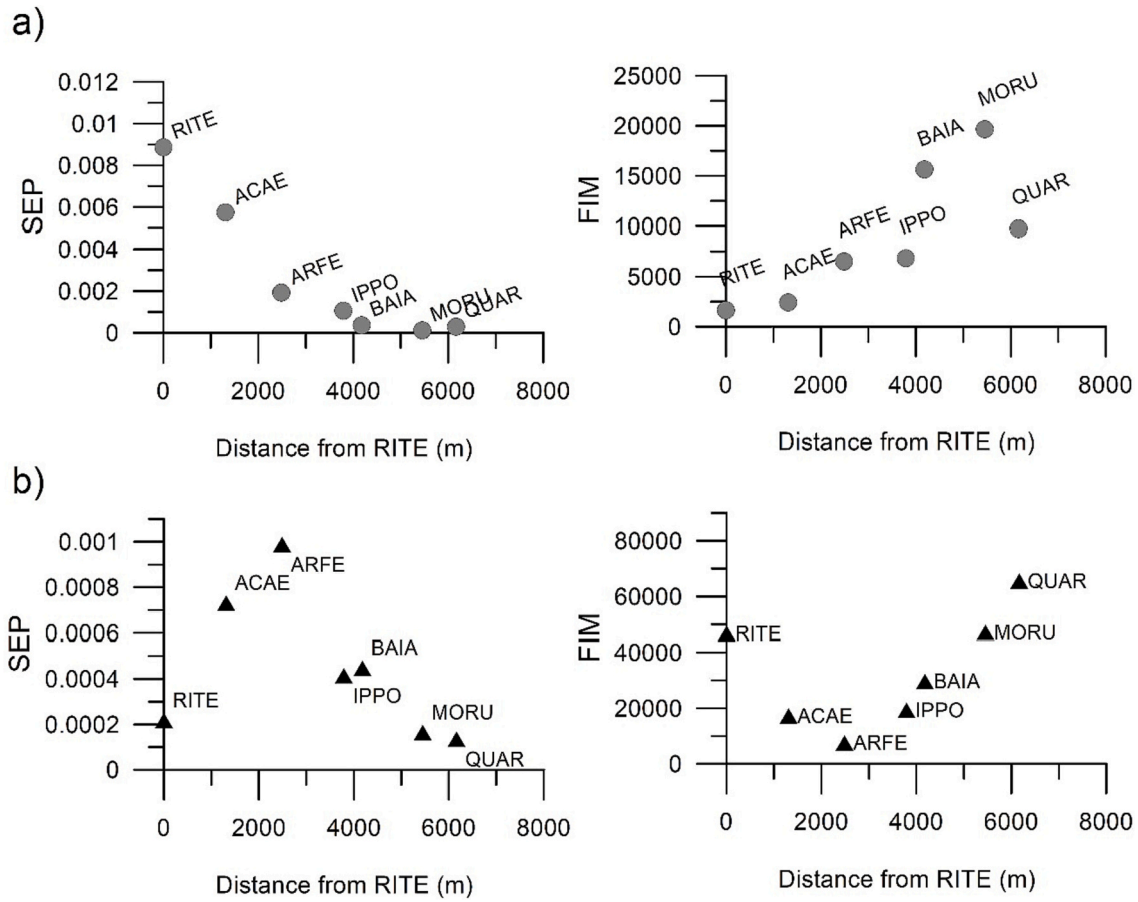

Fig. 2. SEP and FIM of V (a) and H (b) deformation data as a function of distance from RITE station.

by a point in the $FIM{\cdot}SEP \geq 1$; and $FIM{\cdot}SEP = 1$ only for Gaussian processes.

3. Results and discussion

For each data set we calculated the FIM and the SEP. Supposing RITE station the closest to the deformation source, in Fig. 2 the FIM and SEP of each dataset are represented as a function of the distance from RITE.

The FIM and SEP of V component reveal a certain spatial pattern given by a decreasing (increasing) behavior of SEP (FIM) with the distance from the source (in correspondence with the location of RITE station), indicating a more disordered and less organized structure of the time dynamics of the V displacement closer to the source, and more ordered and organized far from it. We can see that the maximum V displacement (around RITE station) corresponds to the maximum SEP and to the minimum FIM. The SEP (FIM) of the H displacement increases (decreases) up to the location of ARFE station (installed at about 2.5 km from RITE) and then inverts this trend decreasing (increasing) with farther stations.

The spatial pattern of the SEP for both the V and H components reproduces the spatial pattern of deformation observed in the past by leveling measurements and recently by GPS data (Berrino et al., 1984; Bianchi et al., 1987; De Martino et al., 2021).

Fig. 3 shows the FSIP (Fisher-Shannon Information Plane) of the V and H components: the stations seem to be well discriminated by the SEP concerning the V displacement, by the FIM concerning the H. Considering that SEP is a global measure and FIM a local measure of the smoothness of the probability density function, SEP is more sensitive to the long-term and higher magnitude variations of the V component, while the FIM reflects better local changes in the H component. This different informational response of the V and H components of ground displacement could be linked to the origin of the deformation at CFc that have been ascribed to magmatic or hydrothermal origin, to the combination of both, and influenced by site-effects such as structural setting and rocks properties.

The time varying (or local) SEP and FIM was calculated by using the method of sliding windows that was commonly employed for spectral and dynamical parameters (Carniel and Di Cecca, 1999). In our study we used a sliding window of one year, calculating the local SEP and FIM by means of the Eqs. (1) and (3) in each consecutive window that had at least 75% of data values. The shift between two consecutive windows was set to one day (that corresponds to one data value); this is done for having enough smoothing among the local SEP and FIM values and evaluate their variation with a good time resolution. Figs. 4a, 4b and 4c show the obtained results. A clear variability characterizes the time pattern of both the informational quantities, suggesting the changing dynamics of the volcanic system between disordered states (high/low SEP/FIM) and ordered ones (low/high SEP/FIM).

Fig. 4a (bottom panel) shows, as an example, the density of four subsets of 1 year long corresponding to the minimum/maximum FIM of the H and V components at RITE station and indicated by labels (Fig. 4a top and middle panels). As it can be clearly seen the density of the data is rather peaked when FIM is maximum and rather wide when it is minimum. This is perfectly in agreement with the definition of FIM that emphasizes the local properties of the probability density function of a series, linked with its derivative. Therefore, for instance, a larger FIM indicates that the distribution of the data is characterized by larger local variation that are reflected in its more peaked shape, which indicates that the underlying system undergoes a more ordered status able to generate more concentrated data.

Most strikingly is the quasi-spike-like behavior of SEP/FIM time pattern, indicating that the volcanic system at CFc changes its status with dynamic transitions. The abrupt transition from one regime to another in volcanic systems has been found in several different volcanoes: at Stromboli volcano, Italy, where abrupt transitions between low and high degassing regimes, linked with the normal strombolian activity, of the order of tens of minutes take place (Ripepe et al., 2002); at Erta Ale, Ethiopia, whose convection regimes are characterized by sudden transitions (Jones et al., 2006); at Dallol, Ethiopia, where the alternation of low and high regimes is more evident in the geothermal activity than in the seismic one (Carniel et al., 2010).

Figs. 4a, 4b and 4c (grey stars) also show the major seismic swarms and the major long period (LP) sequence of events (Tramelli et al. (2022) for more details). In particular six seismic swarms were recorded in the closeness of the caldera that might be realistically correlated with volcanic activity (Tramelli et al., 2022): a) August 22, 2000: a swarm of VT events was recorded, one month after a swarm of hybrid events that lasted for a week; in particular, 90 events with magnitudes between −0.5 and 2.1 were recorded within 7 h; b) October 2006: a shallow long period (LP) activity accompanied by a VT swarm lasted for 1 week; c) September 7, 2012: >180 low-magnitude earthquakes occurred within a time window of almost 3 h; d) October 7, 2015: 33 low magnitude earthquakes were recoded within a time window of almost 2 h; e) March 12, 2018: 42 seismic events were recorded in about 2 h; f) December 5–6, 2019: 34 earthquakes with maximum magnitude Md = 3.1 were recorded in the area of Solfatara/Pisciarelli (see vertical lines in Figs. 4a, 4b and 4c). All the stations are sensitive to these seismic onsets, FIM is roughly inversely proportional to SEP, and it detects the small changes in the original series even better than the SEP. In Figs. 4a, 4b and 4c, the SEP of the V component shows the presence of three distinct time phases. A first phase, from 2000 to the end of 2003, characterized by a decreasing trend, that is more pronounced for RITE, ACAE and ARFE stations. During this phase, the system is undergoing a reduction in the entropic state. Starting from 2004, the SEP of V component for stations located in the outer caldera (QUAR and MORU) do not display clear trend until December 2019, thus they can be considered in a stable state indicating that the deformation source plays a quite negligible role on vertical displacements for these distant stations. Conversely, starting from 2004, the SEP of V component (hereafter SEP V) of all the other stations show an oscillating behavior superimposed on an increasing trend that seems more pronounced for the stations closer to the source. Starting from mid-2012, the SEP V of stations RITE, ARFE and ACAE

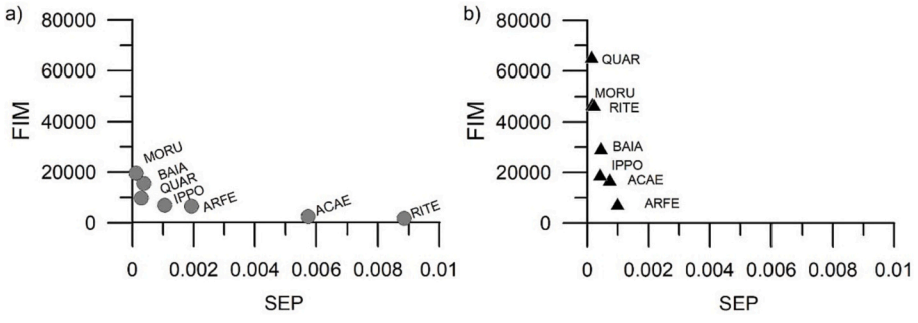

Fig. 3. FSIP of the analyzed V (a) and H (b) data.

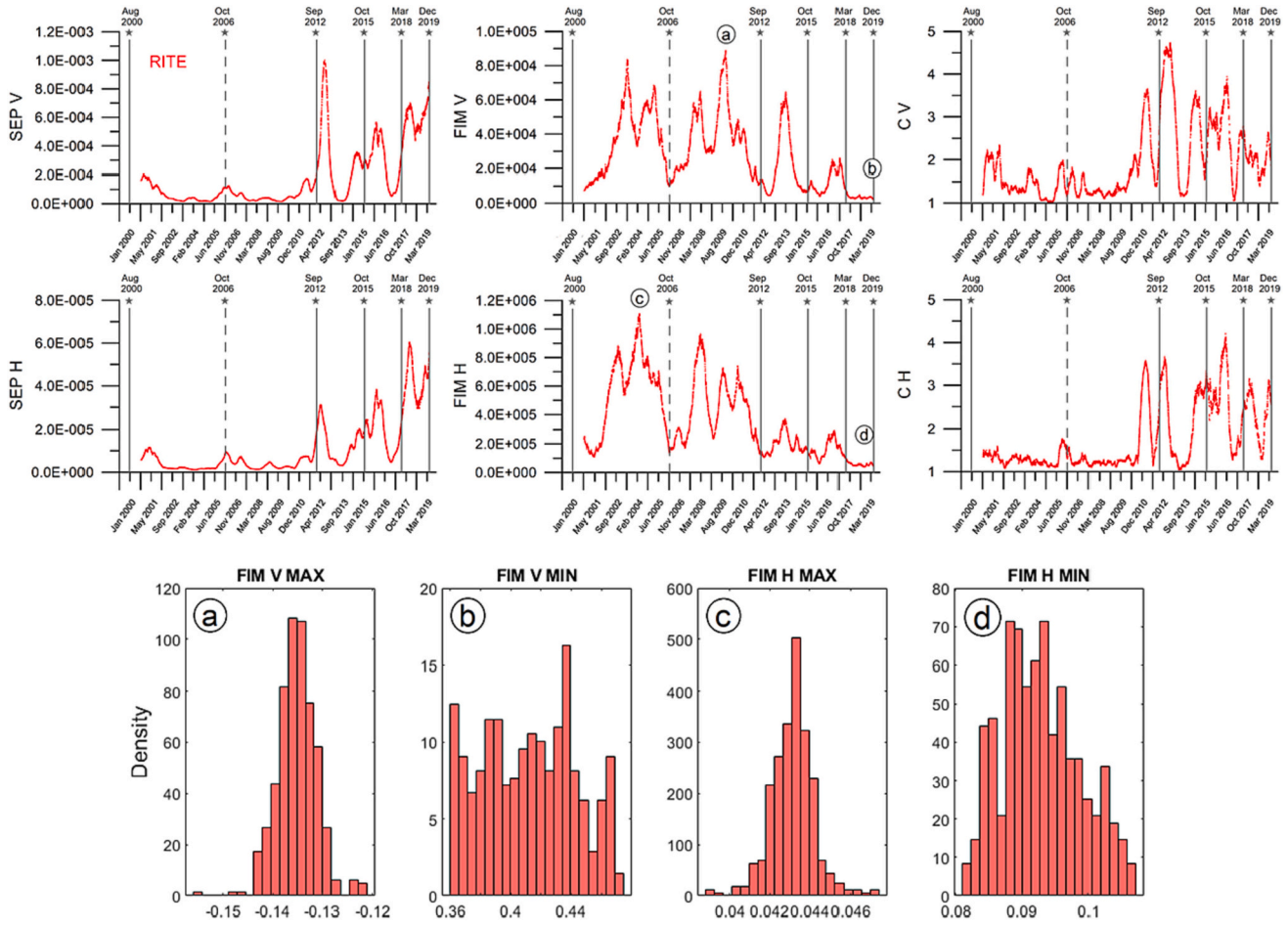

Fig. 4a. Top and middle panels: SEP, FIM and C as a function of time for V (vertical) and H (horizontal) components at station RITE; stars represent seismic swarms (lines) and the major LP swarm (dashed) occurrences. Bottom panel: Density of four subsets corresponding to the minimum/maximum FIM of the H and V components.

show an enhancement of both the trend rise and the peaks' amplitudes, indicating an even stronger change in the dynamics of the deformation source, leading to an enhanced entropic state. Noteworthy, on 7 September 2012 the largest swarm, both in terms of number of earthquakes and released energy, occurred since the end of the bradiseismic crisis of 1982–84, (Tramelli et al., 2022); on the base of the geophysical and geochemical parameters monitored at CFc, the Italian Department of Civil Protection raised the alert level from green to yellow (attention).

From 2000 to 2019 the FIM of the V component (hereafter FIM V) reflects the spatial and temporal pattern of the SEP. However, the drastic change of the SEP in 2012 is less noticeable in the FIM. A clear correspondence between the sharp drops in the FIM (loss of order) and the swarm occurrences, suggests a unique source driving both the occurrence of earthquakes and the vertical displacements. Significant low values of FIM V with time are detected during 2000–2003 indicating a transition period during which the dynamics of the system is losing its order due to a regime change. After 2004, the successive minima of FIM V, can also be interpreted as a response to events that break the order of a certain dynamics and are more pronounced for stations closer to the presumed source.

The SEP of the H component (hereafter SEP H) values are approximately one order of magnitude lower than SEP V values at all stations; the FIM of the H component (hereafter FIM H) values are approximately one order of magnitude higher than FIM V values at all stations. The SEP H and FIM H show similar temporal pattern with respect to their vertical counterparts. The main long-term difference concerns the presence of an increasing SEP H (decreasing FIM H) trend since 2004 also for stations placed in the outer caldera. It seems that the deformation source causes horizontal displacements smaller in magnitude, but persistent in time at larger distances. Similar to the V components, SEP H shows an enhancement of both the trend rise and the oscillation amplitude starting from mid-2012. Again, a clear correspondence between FIM H minima and swarm occurrence is visible, although a greater misalignment of the FIM H minimum peaks from different stations is noted.

Figs. 4a, 4b and 4c show also another informational quantity derived from the FIM and SEP, the so-called complexity C, given by the product of the first two. Concerning the V component, if the two stations located in the outer caldera (MORU, QUAR) do not show significant changes in C throughout the investigated period, the five stations located in the inner caldera (RITE, ACAE, ARFE, IPPO, BAIA) show a clear increase in C starting from 2011. The three stations closer to the caldera center (RITE, ACAE, ARFE) are characterized by larger values of C during all the investigation period with peaks occurring at the same time. The observed spatial pattern reflects the different impact on V displacements with respect to the distance from the deformation source while the observed temporal pattern reflects a change in the dynamics of V displacements after 2011, about one year before the main dynamic changes (mid-2012) well detected by the SEP.

Concerning the H component, the C greatly vary with time at all the recording stations. If no spatial pattern is visible, a certain temporal pattern can be observed; in fact, after 2011 the C is higher on average. It should be noted that before 2011, significant peaks in the C of the H component occur also at stations located far from the caldera center.

As C close to 1 indicates that the time series have a Gaussian

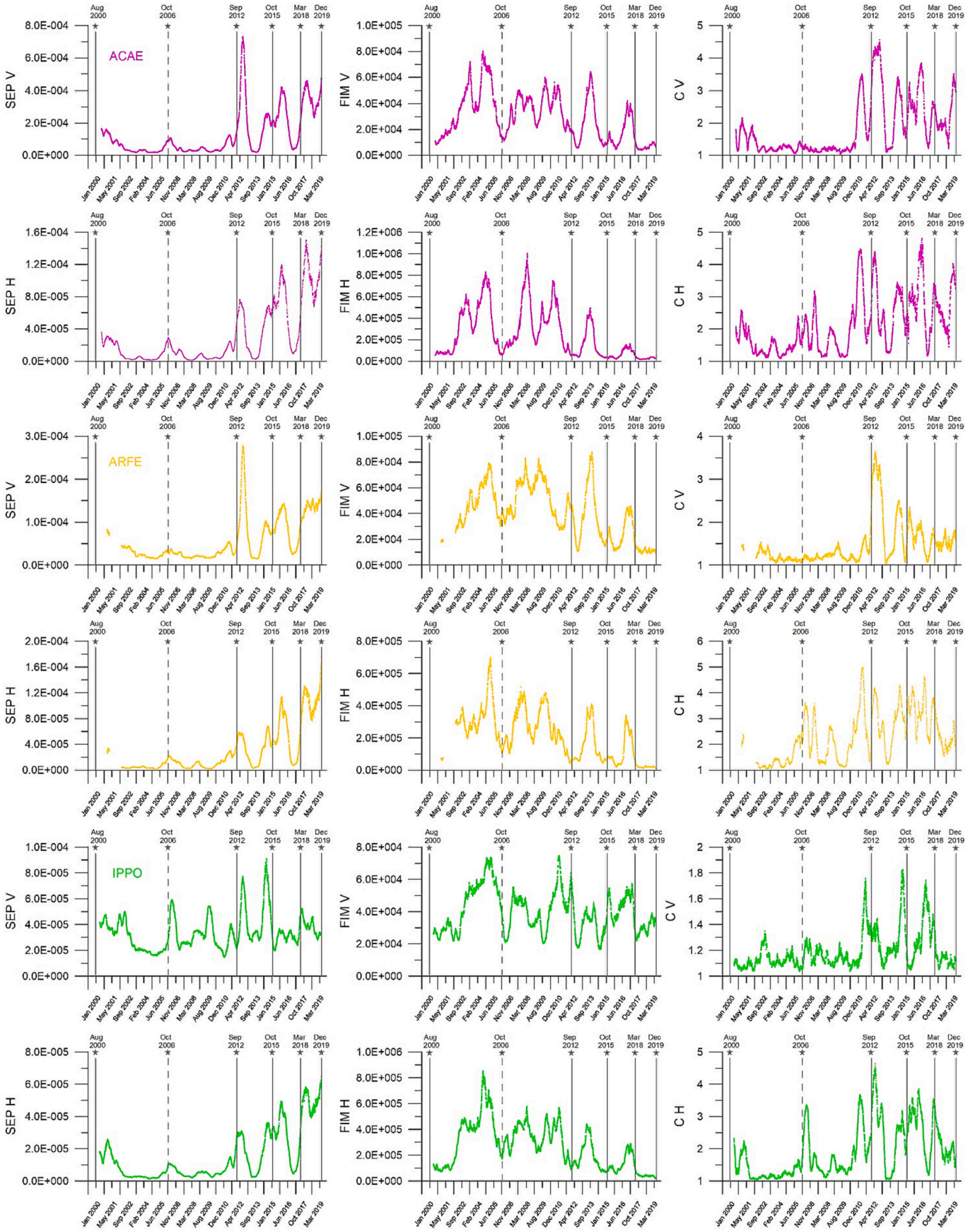

Fig. 4b. SEP, FIM and C as a function of time for V (vertical) and H (horizontal) components at stations ACAE, ARFE, IPPO. Stars represent seismic swarms (lines) and the major LP swarm (dashed) occurrences.

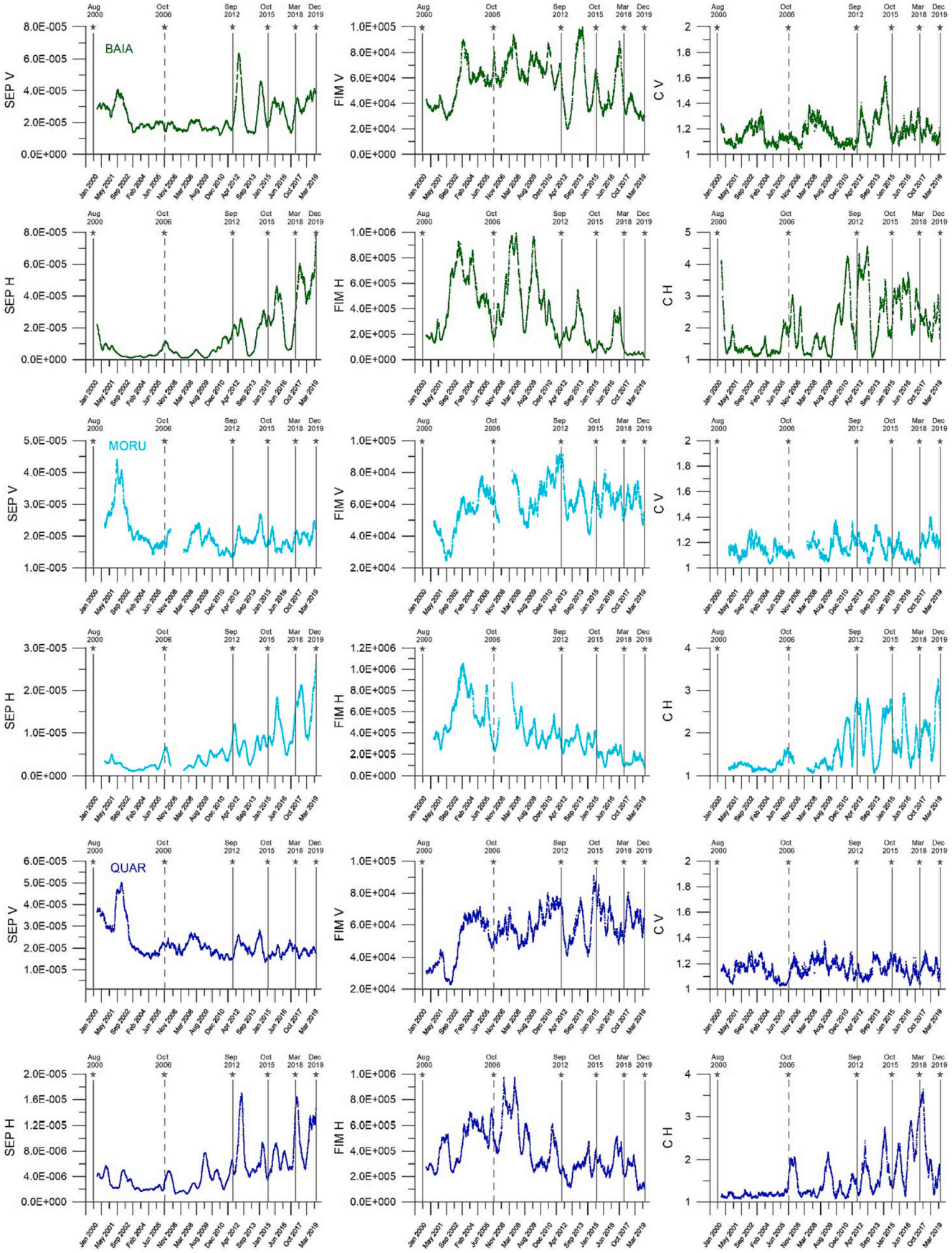

Fig. 4c. SEP, FIM and C as a function of time for V (vertical) and H (horizontal) components at stations BAIA, MORU, QUAR. Stars represent seismic swarms (lines) and the major LP swarm (dashed) occurrences.

distribution, our results indicate that the vertical components of QUAR and MORU stations show a nearly Gaussian distribution during 2000–2019. All other stations and components show a net departure from Gaussianity, indicating that the complexity is very sensible even to small displacement changes and thus to the variations of driving force intensity above some threshold. Thus, C of V and of H components (C V and C H respectively) correlate with the increase of the baseline displacement and to the modulation of small-amplitude displacements. Thus, C V and C H include both global scale variations revealed by SEP information and local scale variations revealed by FIM information.

The behavior of the SEP, FIM, and C of both V and H components in space and time domain poses the problem of evaluating whether it is justified assuming a single source as dominating the signal. However, this task has been faced via different modeling approaches and on different datasets (Amoruso et al., 2014b, Amoruso et al., 2014a and herein references) and can't be addressed here. Here we point to the ability of informational quantities to capture features in the time series to fast and easily track spatial and temporal changes of unpredictable natural dynamics.

4. Conclusion

Analyzing the SEP, FIM and C of the displacement data recorded by the GPS network at CFc, we detected several transitions both in time and space. On global scales the SEP provides information on the dynamics of the deformation source, such as the detection of a spatial pattern, the presence of a fast-rise phase, the small-scale changes in the deformation dynamics. On local scales the FIM well detects periods of disorder that coincide with swarm occurrences, indicating that the system is undergoing internal or external source deformation and volcano/tectonic stress. Global features in the SEP and local features in the FIM complement themselves in the complexity parameter C. The existence of two main different states, well recognized by the long-term and abrupt changes in SEP starting from 2012, is revealed about one year before in the C plot indicating the approaching of the system to a critical threshold. For this examined ground displacement time series, the C complexity could be considered a precursory signal before the system experiences a new state. Our results suggest that the informational properties of GPS signals allow to monitor complex processes and may be useful to detect unpredictable and hazardous dynamic changes as fast as possible.

Declaration of Competing Interest

The authors declare that they have no known competing financial interests or personal relationships that could have appeared to influence the work reported in this paper.

Data availability

Analyzed data are available in De Martino et al. (2021), see text for details.

Acknowledgements

This work was partially supported by Project PRIN n. 201743P29 FLUIDS (Detection and tracking of crustal fluid by multi-parametric methodologies and technologies).

References

Acocella, V., Di Lorenzo, R., Newhall, C., Scandone, R., 2015. An overview of recent (1988 to 2014) caldera unrest: Knowledge and perspectives: CALDERA UNREST. Rev. Geophys. 53, 896–955. https://doi.org/10.1002/2015RG000492.

Amoruso, A., Crescentini, L., Sabbetta, I., 2014a. Paired deformation sources of the Campi Flegrei caldera (Italy) required by recent (1980-2010) deformation history. J. Geophys. Res. Solid Earth 119, 858–879. https://doi.org/10.1002/2013JB010392.

Amoruso, A., Crescentini, L., Sabbetta, I., De Martino, P., Obrizzo, F., Tammaro, U., 2014b. Clues to the cause of the 2011-2013 Campi Flegrei caldera unrest, Italy, from continuous GPS data. Geophys. Res. Lett. 41, 3081–3088. https://doi.org/10.1002/2014GL059539.

Barberi, F., Corrado, G., Innocenti, F., Luongo, G., 1984. Phlegraean Fields 1982–1984: Brief chronicle of a volcano emergency in a densely populated area. Bull. Volcanol. 47, 175–185. https://doi.org/10.1007/BF01961547.

Battaglia, M., Troise, C., Obrizzo, F., Pingue, F., De Natale, G., 2006. Evidence for fluid migration as the source of deformation at Campi Flegrei caldera (Italy): DEFORMATION AT CAMPI FLEGREI CALDERA (ITALY). Geophys. Res. Lett. 33, n/a-n/a. https://doi.org/10.1029/2005GL024904.

Berrino, G., Corrado, G., Luongo, G., Toro, B., 1984. Ground deformation and gravity changes accompanying the 1982 Pozzuoli uplift. Bull. Volcanol. 47, 187–200. https://doi.org/10.1007/BF01961548.

Bianchi, R., Coradini, A., Federico, C., Giberti, G., Lanciano, P., Pozzi, J.P., Sartoris, G., Scandone, R., 1987. Modeling of surface deformation in volcanic areas: the 1970-1972 and 1982-1984 crises of Campi Flegrei, Italy. J. Geophys. Res. 92, 14139–14150. https://doi.org/10.1029/JB092iB13p14139.

Bonafede, M., Mazzanti, M., 1998. Modelling gravity variations consistent with ground deformation in the Campi Flegrei caldera (Italy). J. Volcanol. Geotherm. Res. 81, 137–157. https://doi.org/10.1016/S0377-0273(97)00071-1.

Bottiglieri, M., Falanga, M., Tammaro, U., Obrizzo, F., De Martino, P., Godano, C., Pingue, F., 2007. Independent component analysis as a tool for ground deformation analysis. Geophys. J. Int. 168, 1305–1310. https://doi.org/10.1111/j.1365-246X.2006.03264.x.

Bottiglieri, M., Falanga, M., Tammaro, U., De Martino, P., Obrizzo, F., Godano, C., Pingue, F., 2010. Characterization of GPS time series at the Neapolitan volcanic area by statistical analysis. J. Geophys. Res. 115, B10416. https://doi.org/10.1029/2009JB006594.

Carniel, R., Di Cecca, M., 1999. Dynamical tools for the analysis of long term evolution of volcanic tremor at Stromboli. Ann. Geophys. 42, 10. https://doi.org/10.4401/ag-3732.

Carniel, R., Jolis, E.M., Jones, J., 2010. A geophysical multi-parametric analysis of hydrothermal activity at Dallol, Ethiopia. J. Afr. Earth Sci. 58, 812–819. https://doi.org/10.1016/j.jafrearsci.2010.02.005.

Chen, H.-J., Telesca, L., Lovallo, M., Chen, C.-C., 2021. Unveiling Informational Properties of the Chen-Ouillon-Sornette Seismo-Electrical Model. Entropy 23, 337. https://doi.org/10.3390/e23030337.

D'Auria, L., Giudicepietro, F., Aquino, I., Borriello, G., Del Gaudio, C., Lo Bascio, D., Martini, M., Ricciardi, G.P., Ricciolino, P., Ricco, C., 2011. Repeated fluid-transfer episodes as a mechanism for the recent dynamics of Campi Flegrei caldera (1989–2010). J. Geophys. Res. 116, B04313. https://doi.org/10.1029/2010JB007837.

D'Auria, L., Pepe, S., Castaldo, R., Giudicepietro, F., Macedonio, G., Ricciolino, P., Tizzani, P., Casu, F., Lanari, R., Manzo, M., Martini, M., Sansosti, E., Zinno, I., 2015. Magma injection beneath the urban area of Naples: a new mechanism for the 2012–2013 volcanic unrest at Campi Flegrei caldera. Sci. Rep. 5, 13100. https://doi.org/10.1038/srep13100.

De Lauro, E., Petrosino, S., Ricco, C., Aquino, I., Falanga, M., 2018. Medium and long period ground oscillatory pattern inferred by borehole tiltmetric data: New perspectives for the Campi Flegrei caldera crustal dynamics. Earth Planet. Sci. Lett. 504, 21–29. https://doi.org/10.1016/j.epsl.2018.09.039.

De Martino, P., Tammaro, Umberto, Obrizzo, Francesco, 2014. GPS time series at Campi Flegrei caldera (2000−2013). Ann. Geophys. 57, 2. https://doi.org/10.4401/ag-6431.

De Martino, P., Dolce, M., Brandi, G., Scarpato, G., Tammaro, U., 2021. The Ground Deformation History of the Neapolitan Volcanic Area (Campi Flegrei Caldera, Somma–Vesuvius Volcano, and Ischia Island) from 20 Years of Continuous GPS Observations (2000–2019). Remote Sens. 13, 2725. https://doi.org/10.3390/rs13142725.

De Natale, G., Pingue, F., 1993. Ground deformations in collapsed caldera structures. J. Volcanol. Geotherm. Res. 57, 19–38. https://doi.org/10.1016/0377-0273(93)90029-Q.

De Natale, G., Zollo, Aldo, 1986. Statistical analysis and clustering features of the Phlegraean Fields earthquake sequence (May 1983-May 1984). Bull. Seismol. Soc. Am. 801–814.

De Vivo, B., Rolandi, G., Gans, P.B., Calvert, A., Bohrson, W.A., Spera, F.J., Belkin, H.E., 2001. New constraints on the pyroclastic eruptive history of the Campanian volcanic Plain (Italy). Mineral. Petrol. 73, 47–65. https://doi.org/10.1007/s007100170010.

Deino, A.L., Orsi, G., de Vita, S., Piochi, M., 2004. The age of the Neapolitan Yellow Tuff caldera-forming eruption (Campi Flegrei caldera – Italy) assessed by 40Ar/39Ar dating method. J. Volcanol. Geotherm. Res. 133, 157–170. https://doi.org/10.1016/S0377-0273(03)00396-2.

Del Gaudio, C., Aquino, I., Ricciardi, G.P., Ricco, C., Scandone, R., 2010. Unrest episodes at Campi Flegrei: a reconstruction of vertical ground movements during 1905–2009. J. Volcanol. Geotherm. Res. 195, 48–56. https://doi.org/10.1016/j.jvolgeores.2010.05.014.

Devroye, L., 1987. A Course in Density Estimation. Progress in probability and statistics, Birkhäuser, Boston.

Dong, D., Fang, P., Bock, Y., Cheng, M.K., Miyazaki, S., 2002. Anatomy of apparent seasonal variations from GPS-derived site position time series: SEASONAL VARIATIONS FROM GPS SITE TIME SERIES. J. Geophys. Res. 107 https://doi.org/10.1029/2001JB000573. ETG 9-1-ETG 9-16.

Dvorak, J.J., Dzurisin, D., 1997. Volcano geodesy: the search for magma reservoirs and the formation of eruptive vents. Rev. Geophys. 35, 343–384. https://doi.org/10.1029/97RG00070.

Dvorak, J.J., Mastrolorenzo, G., 1991. The mechanisms of recent vertical crustal movements in Campi Flegrei caldera, southern Italy. Geological Society of America. https://doi.org/10.1130/SPE263.

Esquivel, R.O., Angulo, J.C., Antolín, J., Dehesa, J.S., López-Rosa, S., Flores-Gallegos, N., 2010. Analysis of complexity measures and information planes of selected molecules in position and momentum spaces. Phys. Chem. Chem. Phys. 12, 7108. https://doi.org/10.1039/b927055h.

Frieden, B.R., 1990. Fisher information, disorder, and the equilibrium distributions of physics. Phys. Rev. A 41, 4265–4276. https://doi.org/10.1103/PhysRevA.41.4265.

Gaeta, F.S., 2003. A physical appraisal of a new aspect of bradyseism: the miniuplifts. J. Geophys. Res. 108, 2363. https://doi.org/10.1029/2002JB001913.

Gualandi, A., Serpelloni, E., Belardinelli, M.E., 2016. Blind source separation problem in GPS time series. J. Geod. 90, 323–341. https://doi.org/10.1007/s00190-015-0875-4.

Guignard, F., Laib, M., Amato, F., Kanevski, M., 2020. Advanced analysis of temporal data using fisher-shannon information: theoretical development and application in geosciences. Front. Earth Sci. 8, 255. https://doi.org/10.3389/feart.2020.00255.

Janicki, A., Weron, A., 1994. Simulation and Chaotic Behavior of [Alpha]-Stable Stochastic Processes, Monographs and Textbooks in Pure and Applied Mathematics. M. Dekker, New York.

Jones, J., Carniel, R., Harris, A.J.L., Malone, S., 2006. Seismic characteristics of variable convection at Erta 'Ale lava lake, Ethiopia. J. Volcanol. Geotherm. Res. 153, 64–79. https://doi.org/10.1016/j.jvolgeores.2005.08.004.

Lima, A., De Vivo, B., Spera, F.J., Bodnar, R.J., Milia, A., Nunziata, C., Belkin, H.E., Cannatelli, C., 2009. Thermodynamic model for uplift and deflation episodes (bradyseism) associated with magmatic–hydrothermal activity at the Campi Flegrei (Italy). Earth Sci. Rev. 97, 44–58. https://doi.org/10.1016/j.earscirev.2009.10.001.

Lovallo, M., Marchese, F., Pergola, N., Telesca, L., 2007. Fisher information analysis of volcano-related advanced, very-high-resolution radiometer (AVHRR) thermal products time series. Physica A: Statistical Mechanics and its Applications 384, 529–534. https://doi.org/10.1016/j.physa.2007.05.066.

Lovallo, M., Marchese, F., Pergola, N., Telesca, L., 2009. Fisher information measure of temporal fluctuations in satellite advanced very high resolution radiometer (AVHRR) thermal signals recorded in the volcanic area of Etna (Italy). Commun. Nonlinear Sci. Numer. Simul. 14, 174–181. https://doi.org/10.1016/j.cnsns.2007.07.006.

Moreno-Torres, L.R., Gomez-Vieyra, A., Lovallo, M., Ramírez-Rojas, A., Telesca, L., 2018. Investigating the interaction between rough surfaces by using the Fisher–Shannon method: Implications on interaction between tectonic plates. Physica A: Statistical Mechanics and its Applications 506, 560–565. https://doi.org/10.1016/j.physa.2018.04.023.

Parascandola, A., 1947. I fenomeni bradisismici del Serapeo di Pozzuoli. Stab. Tipogr. G, Genovese, Napoli.

Petrillo, Z., D'Auria, L., Mangiacapra, A., Chiodini, G., Caliro, S., Scippacercola, S., 2019. A perturbative approach for modeling short-term fluid-driven ground deformation episodes on volcanoes: a case study in the campi flegrei Caldera (Italy). J. Geophys. Res. Solid Earth 124, 1036–1056. https://doi.org/10.1029/2018JB015844.

Petrosino, S., Cusano, P., Madonia, P., 2018. Tidal and hydrological periodicities of seismicity reveal new risk scenarios at Campi Flegrei caldera. Sci. Rep. 8, 13808. https://doi.org/10.1038/s41598-018-31760-4.

Raykar, V.C., Duraiswami, R., 2006. Fast optimal bandwidth selection for kernel density estimation. In: Presented at the Proceedings of the SIAM International Conference on Data Mining, pp. 524–528.

Ricco, C., Petrosino, S., Aquino, I., Del Gaudio, C., Falanga, M., 2019. Some investigations on a possible relationship between ground deformation and seismic activity at campi flegrei and ischia volcanic areas (southern Italy). Geosciences 9, 222. https://doi.org/10.3390/geosciences9050222.

Ripepe, M., Harris, A.J.L., Carniel, R., 2002. Thermal, seismic and infrasonic evidences of variable degassing rates at Stromboli volcano. J. Volcanol. Geotherm. Res. 118, 285–297. https://doi.org/10.1016/S0377-0273(02)00298-6.

Shannon, C.E., 1948. A Mathematical Theory of Communication. Bell System Technical Journal 27, 379–423. https://doi.org/10.1002/j.1538-7305.1948.tb01338.x.

Telesca, L., Lovallo, M., 2017. On the performance of fisher information measure and shannon entropy estimators. Physica A: Statistical Mechanics and its Applications 484, 569–576. https://doi.org/10.1016/j.physa.2017.04.184.

Telesca, L., Lapenna, V., Lovallo, M., 2005. Fisher Information Analysis of earthquake-related geoelectrical signals. Nat. Hazards Earth Syst. Sci. 5, 561–564. https://doi.org/10.5194/nhess-5-561-2005.

Telesca, L., Lovallo, M., Carniel, R., 2010. Time-dependent Fisher Information measure of volcanic tremor before the 5 April 2003 paroxysm at Stromboli volcano, Italy. J. Volcanol. Geotherm. Res. 195, 78–82. https://doi.org/10.1016/j.jvolgeores.2010.06.010.

Telesca, L., Lovallo, M., Martì Molist, J., López Moreno, C., Abella Meléndez, R., 2014a. Using the Fisher-Shannon method to characterize continuous seismic signal during volcanic eruptions: application to 2011-2012 El Hierro (Canary Islands) eruption. Terra Nova 26, 425–429. https://doi.org/10.1111/ter.12114.

Telesca, L., Lovallo, M., Romano, G., Konstantinou, K.I., Hsu, H.-L., Chen, C., 2014b. Using the informational Fisher–Shannon method to investigate the influence of long-term deformation processes on geoelectrical signals: An example from the Taiwan orogeny. Physica A: Statistical Mechanics and its Applications 414, 340–351. https://doi.org/10.1016/j.physa.2014.07.060.

Todesco, M., Rinaldi, A.P., Bonafede, M., 2010. Modeling of unrest signals in heterogeneous hydrothermal systems. J. Geophys. Res. 115, B09213. https://doi.org/10.1029/2010JB007474.

Tramelli, A., Giudicepietro, F., Ricciolino, P., Chiodini, G., 2022. The seismicity of Campi Flegrei in the contest of an evolving long term unrest. Sci. Rep. 12, 2900. https://doi.org/10.1038/s41598-022-06928-8.

Trasatti, E., Polcari, M., Bonafede, M., Stramondo, S., 2015. Geodetic constraints to the source mechanism of the 2011–2013 unrest at Campi Flegrei (Italy) caldera. Geophys. Res. Lett. 42, 3847–3854. https://doi.org/10.1002/2015GL063621.

Tripaldi, S., Scippacercola, S., Mangiacapra, A., Petrillo, Z., 2020. Granger Causality Analysis of Geophysical, Geodetic and Geochemical Observations during Volcanic Unrest: a Case Study in the Campi Flegrei Caldera (Italy). Geosciences 10, 185. https://doi.org/10.3390/geosciences10050185.

Troise, C., De Natale, G., Schiavone, R., Somma, R., Moretti, R., 2019. The Campi Flegrei caldera unrest: Discriminating magma intrusions from hydrothermal effects and implications for possible evolution. Earth Sci. Rev. 188, 108–122. https://doi.org/10.1016/j.earscirev.2018.11.007.

Troudi, M., Alimi, A.M., Saoudi, S., 2008. Analytical plug-in method for kernel density estimator applied to genetic neutrality study. EURASIP J. Adv. Signal Process. 2008, 739082 https://doi.org/10.1155/2008/739082.

Wu, T.-H., Chen, C.-C., Lovallo, M., Telesca, L., 2019. Informational analysis of Langevin equation of friction in earthquake rupture processes. Chaos 29, 103120. https://doi.org/10.1063/1.5092552.